Preclinical and clinical validation of a novel oxygenation imaging system

Sylvain Gioux[1,*,†], Amaan Mazhar[5,6*], Bernard T. Lee [2], David J. Cuccia[3], Alan Stockdale[1], Rafiou Oketokoun[1], Yoshimoto Ashitate[1,4], Nicholas Durr[1], Anthony J. Durkin[6], Bruce J. Tromberg[5,6], John V. Frangioni[1]

[1]Division of Hematology/Oncology, Dept. of Medicine and Dept. of Radiology, [2]Division of Plastic and Reconstructive Surgery Beth Israel Deaconess Medical Center, Boston, MA 02215
[3]Modulated Imaging Inc. Technology Incubator Office 1002 Health Sciences Road Irvine, California 92612
[4]Division of Cancer Diagnostics and Therapeutics, Hokkaido University Graduate School of Medicine, Sapporo, Japan
[5]Dept. of Biomedical Engineering University of California, Irvine
[6]Beckman Laser Institute 1002 Health Sciences Road Irvine, California 92612

[*]Both authors contributed equally to the study

ABSTRACT

Introduction: Two major disadvantages of currently available oxygenation probes are the need for contact with the skin and long measurement stabilization times. A novel oxygenation imaging device based on spatial frequency domain and spectral principles has been designed, validated preclinically on pigs, and validated clinically on humans. Importantly, this imaging system has been designed to operate under the rigorous conditions of an operating room. Materials and Methods: Optical properties reconstruction and wavelength selection have been optimized to allow fast and reliable oxyhemoglobin and deoxyhemoglobin imaging under realistic conditions. *In vivo* preclinical validation against commercially available contact oxygenation probes was performed on pigs undergoing arterial and venous occlusions. Finally, the device was used clinically to image skin flap oxygenation during a pilot study on women undergoing breast reconstruction after mastectomy. Results: A novel illumination head containing a spatial light modulator (SLM) and a novel fiber-coupled high power light source were constructed. Preclinical experiments showed similar values between local probes and the oxygenation imaging system, with measurement times of the new system being < 500 msec. During pilot clinical studies, the imaging system was able to provide near real-time oxyHb, deoxyHb, and saturation measurements over large fields of view (> 300 cm^2). Conclusion: A novel optical-based oxygenation imaging system has the potential to replace contact probes during human surgery and to provide quantitative, wide-field measurements in near real-time.

Keywords: Oxygenation, Spatial Frequency Domain Imaging, Image-Guided Surgery, Clinical Translation, Optical Imaging Systems, Multispectral Imaging, Diffuse Optical Imaging

[†]Email: sgioux@bidmc.harvard.edu

1. INTRODUCTION

The introduction of pulse oxymetry in the 1970s revolutionized interventional medicine by providing the surgeon with patient status feedback in real-time. [1,2] Pulse oxymetry is based on the measurement of light attenuation as a function of time, and allows for pulse rate and measurement of arterial oxygen saturation. New developments following progress in modeling light-tissue interactions have led to the introduction of local spectroscopic probes capable of determining total oxygen saturation and the blood constituent concentration of oxyhemoglobin and deoxyhemoglobin [3,4]. However, these probes only provide local measurements, which require the surgeon to have prior knowledge of the location of a potential problem. This limitation prevents the use of these probes as passive monitoring devices during surgery. Therefore, surgeons must still rely on visual inspection to diagnose potential problems.

A passive method of monitoring oxygen saturation and oxyhemoglobin and deoxyhemoglobin concentration would aid surgeons in improving patient management. Using these parameters, the surgeon would be able to intervene intraoperatively to prevent damage otherwise not identified. Multispectral imaging of the optical properties of tissue (namely absorption and reduced scattering coefficients, μ_a and μ_s) can determine vital tissue parameters by deconvolving the contribution of each tissue constituent or chromophore, based on their specific absorption spectrum. [3,5,6] Spatial Frequency Domain Imaging (SFDI) is a novel non-contact imaging technique capable of extracting tissue optical properties rapidly and over large fields of view (typically > 5cm). [7,8] By performing multispectral SFDI measurements, optical properties are measured at various wavelengths and tissue chromophores can be determined.

In this study, we present a novel oxygenation-imaging device based on multispectral SFDI acquisition that allows for the determination of tissue chromophores in clinically realistic conditions. We validated the oxygenation-imaging capabilities of the system preclinically by performing venous occlusion of a Yorkshire pig skin flap and then comparing the oxygen saturation results from those obtained with an FDA-approved local oxygenation probe. Finally, we translated the imaging system to the clinic and performed the first-in-human skin flap oxygenation imaging for patients undergoing breast reconstruction after mastectomy. This study lays the foundation for clinical translation of endogenous chromophore imaging in surgery.

2. MATERIALS AND METHODS

2.1 Spatial frequency domain imaging (SFDI)

Although extensive details about spatial frequency domain imaging (SFDI) have been previously published, [7-19] a short description is provided here. The spatial variation of the diffuse reflectance from a point illumination is dependent upon the optical properties of the medium. [20] The characterization of this variation, sometimes called spatial point spread function (s-PSF), allows the determination of medium optical properties. SFDI relies on the analysis of the Fourier equivalent of the s-PSF, which is the spatial modulation transfer function (s-MTF). [8] The main advantage of working in the spatial frequency domain is that large fields of view can be acquired and processed at once, which is particularly desirable for real-time intraoperative imaging.

We used the method described by Cuccia et al. [8] in which only 2 spatial frequencies (0 mm^{-1} and 0.2 mm^{-1}) are needed to separate absorption from scattering, and the AC component of the intensity sinusoidal wave was extracted using 3 offset phases per frequency. A lookup table (LUT) method was used to compute the optical properties in real-time. We chose to perform one additional phase profilometry acquisition to extract the surface profile and correct for its effect on the measured intensity as previously described [13].

2.2 The imaging system

We based our developments on the Fluorescence-Assisted Resection and Exploration (FLARE^{TM}) imaging system developed in our laboratory for clinical continuous wave (CW) fluorescence measurements. Extensive details regarding the FLARE^{TM} imaging system have been previously described [21,22]. In short, the system consists of a cart containing electronics, a mast, and an arm holding the imaging head, which is positioned over the patient. The imaging head contains an illumination unit, which delivers light onto the surgical field and a collection unit that is capable of simultaneously imaging color video and two video channels of near-infrared (NIR) light. For the purpose of this study, we redesigned the illumination unit to illuminate the surgical field with structured illumination at 6 different wavelengths

(670, 730, 760, 808, 860, and 980 nm). These wavelengths were selected to allow for fast and reliable imaging as described by Mazhar et al. [18] The filtration scheme on the collection unit was also changed to allow for endogenous contrast imaging and consists of 3 channels: color (below 680 nm), NIR1 (between 680 and 770 nm), and NIR2 (above 770 nm). This way, the 6 wavelengths are split equally between the NIR1 camera and the NIR2 camera.

We chose to base our NIR light source design on a remote lighting strategy in which the light source is positioned away from the illumination unit and light is propagated using an optical fiber. To achieve this goal, laser diodes where chosen as the source technology because they are powerful, available at many wavelengths, and are easily coupled into small size optical fiber due to their low etendue. Twelve different diodes were purchased from RPMC Lasers, Inc. (O'Fallon, MO), manufactured by LDX optronics (Maryville, TN), and fiber-coupled into 300 μm, 0.37 NA fibers using custom tuned couplers with integrated thermoelectric coolers (TEC) purchased from OZOptics (Ottawa, Ontario). Each fiber leg is a part of a 12-to-1 multifiber bundle purchased from Ceramoptec (East Longmeadow, MA) that combined all fibers into a 1.33 mm FC output. Each diode was controlled in intensity and temperature using a Thorlabs (Newton, New Jersey) OEM controller with ± 3 A current driving capability for both the diode and the TEC (model# ITC133). Power was supplied with two 900 W AC-DC power supplies model # ACE9-QQWWWW-00-H (COSEL, Toyama, Japan), and the whole light source was packaged into a custom-made enclosure from OZoptics.

The illumination unit provided both planar CW NIR-depleted white light for the surgical procedure and NIR structured illumination for SFDI measurements. White light was provided from 18 rebel LED white light modules capable of projecting more than 40,000 lux of NIR-depleted light during surgery, as previously described [21]. NIR light is propagated from the remote light source into a 0.7-inch XGA (1024 x 768 pixel resolution) digital light projector (DLP; GFM, Berlin, Germany, model Alligator) purchased from Modulated Imaging Inc. (Irvine, CA). Patterns from the digital micro-mirror device (DMD) are projected using NIR compatible optics (Carl Zeiss, Oberkochen, Germany, model NIR S2+) and purchased from Modulated Imaging Inc. (Irvine, CA).

The collection unit was identical to the one used for the FLARE[TM] imaging system. In short, it consists of one color camera (model no. Imitech IMC-80F, IMI Technology, Seoul, Korea), and two NIR cameras (model no. Orca-AG, Hamamatsu, Bridgewater, New Jersey). The only difference was regarding filtration, which allowed for endogenous contrast imaging as follows: a 650 nm short pass filter was used in front of the color camera to clean up the NIR illumination, a 655nm long pass filter was used in front of the NIR1 camera, and a 785nm long pass filter was used in front of the NIR2 camera.

2.3 SFDI acquisition and processing

SFDI acquisitions were performed as previously described, [8,13] but with 2 NIR cameras collecting images simultaneously with color video. In short, each NIR camera acquired one of two simultaneously projected wavelengths. NIR1 camera acquired three shorter wavelengths (670, 730, and 760 nm) sequentially while NIR2 simultaneously acquired three longer wavelengths (808, 860, and 980 nm) sequentially. The wavelengths can be paired as desired by the user. The typical sequence of events to perform SFDI measurements consisted of the following: 1.) Calibration: Profile correction required a multi-height calibration to be performed. In short, the system was positioned at 18 inches (45 cm) from the imaging plane and the reference optical phantom was acquired from -2 cm to +2 cm of vertical translation relative to the imaging plane; 2.) Acquisition: Profile corrected SFDI acquisition consisted of a single wavelength profile acquisition using the 650 nm immediately followed by an optical properties measurement with 2 spatial frequencies: 0 mm^{-1} and 0.2 mm^{-1}. During acquisition in the operating room, the entire system was wrapped in a sterile shield and drape (Medical Technique Inc., Tucson, AZ); 3.) Processing: Images were post-processed to extract optical properties at all acquired wavelengths to determine chromophore content. All acquisitions were performed using custom written software in C# language designed by Modulated Imaging Inc. Processing was done using software written in MATLAB (Mathworks, Natick, MA).

2.4 Oxygenation measurement reference device

An FDA-approved spectroscopic local probe was used for intraoperative oxygenation measurement. The Vioptix T.Ox (Tissue Oxymeter) is a contact probe with 2 sources (690 and 830 nm) and 2 detectors that measure tissue oxygenation (arterial & venous). It has mainly been used in reconstructive surgery to predict flap viability [23,24] and is an appropriate technology to compare with SFDI.

2.5 Animal experiments

In vivo validation and comparative study was performed during venous occlusion of skin flaps on large animals. Yorkshire pigs (n=3) weighing approximately 30 kg and of either sex were purchased from E. M. Parsons and Sons (Hadley, Massachusetts). Anesthesia was induced using 4.4 mg/kg intramuscular Telazol (Fort Dodge Labs, Fort Dodge, Iowa), and maintained through a 7-mm endotracheal tube with 1.5% isoflurane/balance O_2 at 5 L/min.

The pedicled abdominal flaps were designed to encompass the deep superior epigastric artery (DSEA) and deep superior epigastric vein (DSEV). We created vascular occlusion models by clamping the DSEA or DSEV using bulldog clamps. Five min of baseline acquisition was performed, followed by 17 min occlusion and 8 min recovery. Oxygenation was recorded simultaneously using SFDI and the local oxygenation probe. The SFDI system was placed 18 inches away from the skin flap and acquired continuously during the time of the experiment. A Vioptix local oxygenation probe was placed on the occluded flap and covered with black tape to prevent light contamination from the SFDI system NIR illumination. Tissue saturation values were recorded synchronized with those of SFDI.

After each study, anesthetized pigs were euthanized by rapid intravenous injection of 10 ml of Fatal-Plus (Vortech Pharmaceuticals, Dearborn, Michigan).

2.6 First-in-human clinical trial

All patients gave informed consent and were anonymized. Clinical trial participants were women undergoing unilateral or bilateral mastectomy and reconstruction with a microsurgical deep inferior epigastric perforator (DIEP) flap.

Before flap elevation, the SFDI system was positioned 18 inches over one side of the abdomen and NIR acquisition was performed. The contralateral side of the abdomen was imaged in an identical fashion. In this feasibility study results from the SFDI system were not accessible to the operating surgeons, thereby not changing the standard of care that patients received during surgery.

After dissection of the vessels through the intramuscular course and isolation of the selected perforator vessels and vascular pedicle, the flap was imaged at the abdomen prior to transfer. The flap was then transferred to the chest and a microsurgical anastomosis was performed of the deep inferior epigastric artery and vein to the internal mammary vessels. A final assessment was performed using SFDI. Patients were evaluated for complications 1 and 6 weeks after surgery as part of regular postoperative follow up.

3. RESULTS

3.1 The imaging system

A schematic of the imaging system is presented in Fig. 1(a). Light exiting from the light source was projected onto the field of view in the form of patterns using the DMD. Light was collected by an objective lens and split in 3 spectral bands using 2 dichroic mirrors (D1 and D2) below 650 nm on the color camera, between 670 and 800 nm on NIR1 camera, and above 800 nm on NIR2 camera. Note that two linear polarizers were used to reduce the influence of specular reflections. A picture of the clinically compatible imaging system is shown in Fig. 1(b). The system is composed of a cart containing control electronics, computer, light source, mast, and an arm holding the imaging head, which allows for positioning with 6 degrees of adjustability. Note the similarity with the FLARE[TM] imaging system as only the illumination unit has been modified. The bottom view of the illumination unit is shown in Figure 1(c). Note the 18 white light modules arranged on a spherical cap to allow for optimal illumination uniformity. [21] The projection optics of the DMD were located at the top of the unit. Finally, a cone aperture was used to avoid collecting specular reflections from the surrounding white light sources reflecting on the sterile shield.

A schematic of the light source is presented in Fig. 2(a). Control electronics communicate with the computer through a USB-to-serial interface. Diode modules can be turned on or off, and the diode intensity can be adjusted. Each diode module was composed of one laser diode, a thermoelectric cooler (TEC) with heatsink, and a FC coupler. A 12-to-1 fiber bundle was used to combine all wavelengths together onto a single FC connector. A picture of the actual open assembly is shown in Fig. 2(b). All diode modules and controllers were fit in a custom-made enclosure. Note the diode modules and the 12-to-1 fiber bundle.

3.2 Animal experiments

Results from animal experiments are shown in Fig. 3. Color images (left) and SFDI oxygen saturation (StO_2) images (right) before venous occlusion (t = 0 min, top), during venous occlusion (t = 20 min, middle), and after release (t = 30 min, bottom) are shown in Fig. 3(a). Note, a purple discoloration of the tissue was observed in the color image during occlusion as blood pooled in the tissue. The decrease of oxygen saturation was clearly noticeable in the SFDI images. Time plots of oxygenation saturation (StO_2, top) were taken using the Vioptix probe and SFDI. Time plots of oxyhemoglobin (middle) and deoxyhemoglobin (bottom), were taken using SFDI, as shown in Fig. 3(b). The values plotted from SFDI measurements were mean values from a region of interest on the skin flap (black dashed square in Fig. 3(a)). The oxygenation probe result and the SFDI measurement were similar. Oxyhemoglobin and deoxyhemoglobin traces show an accumulation of each chromophore during occlusion, indicating an increase in blood volume consistent with physiological expectations seen in venous thrombosis.

3.3 First-in-human clinical trial

The clinical trial was approved by the Institutional Review Board (IRB) of the Beth Israel Deaconess Medical Center and was performed in accordance with the ethical standards of the Helsinki Declaration of 1975. The IRB deemed the SFDI imaging system a "non-significant risk" device. Trained personnel easily installed the imaging system in the operating room. The system was draped in a sterile fashion using a shield/drape combination that can be applied by a single person. After draping, the imaging head entered the sterile field and was positioned at a fixed distance. Images were acquired to extract profile information and optical properties at several wavelengths, as described previously.

SFDI measurements are shown in Fig. 4, taken during the bilateral TRAM procedure. From left to right, preparation of the flap (Preparation), flap after elevation (Elevation), and after surgical attachment (Transplant). Extracted maps of oxyhemoglobin concentration (top), deoxyhemoglobin concentration (middle), and tissue saturation (bottom) are presented for each step of the procedure. There was a significant decrease in saturation only after transplantation. After elevation, the saturation value remained almost constant while a significant decrease in both oxyhemoglobin and deoxyhemoglobin was observed. This figure illustrates a case where oxygen saturation measurement did not indicate a decrease in tissue perfusion. The artifacts on the images are due to phase unwrapping issues in the profile correction.

4. DISCUSSION

The presented imaging system was translated to the clinic and used during the clinical trial for patients undergoing breast reconstruction after mastectomy. In order to provide useful intraoperative feedback to surgeons, the system should be able to display oxygenation images of large areas in real-time. The current illumination field of view is 20 cm x 15 cm and the collection field of view is 16 cm x 12 cm. Such fields of view are similar to those of the FLARE[TM] imaging system and, from our experience, seem to fit well with surgeon needs. The SFDI is a scalable field-of-view technology and can be adjusted as needed. The acquisition time is critical to permit real-time intraoperative imaging. Currently, acquiring 6 wavelengths takes up to 3.6 s, including 2.8 s of acquisition for the 980 nm channel due to poor CCD sensitivity. Recent work by Mazhar et al. [18] has shown that it was possible to image oxygenation reliably using only 2 wavelengths, which reduces the acquisition to 500 ms. Short measurement times used with an inverse-lookup table and on-the-fly processing could lead to a frame rate on the order of 1 frame per s for tissue oxygenation imaging.

Our imaging system could be enhanced in several ways. In particular, an improved profile acquisition method using multiple projection patterns could eliminate phase unwrapping issues and improve the quality of the SFDI oxygenation images. A faster acquisition rate using fewer patterns, reduced spectral content, and increased light throughput can limit issues due to patient movement. Acquisitions at only one frequency can be used to measure the AC and DC component of a projected sinusoidal wave. [11] In addition, profile and optical property data acquisition can be acquired with the same pattern sequence. Finally, Graphics Processing Unit (GPU) enabled data processing can accelerate the visualization step of the data analysis. [25] We estimate that these improvements can increase the frame rate to about 5 frames per s.

5. CONCLUSION

We have designed, constructed, and validated a novel oxygenation-imaging device working in the spatial frequency domain. The system employs a novel laser diode light source capable of providing 6 different wavelengths at high power, a DMD-based projection unit to project patterns of light, and a 3-camera system capable of simultaneously collecting 2 NIR spectral bands with a color image. The imaging system has been validated preclinically during a skin flap occlusion procedure on Yorkshire pigs by comparing the oxygenation values from SFDI to those obtained with a FDA-approved local oxygenation probe. Finally, the system has been translated into the clinic and used for patients undergoing breast reconstruction after mastectomy for flap oxygenation measurements. This study lays the foundation for the clinical translation of oxygenation imaging using multispectral SFDI.

ACKNOWLEDGEMENTS

REFERENCES:

[1] Mendelson, Y., "Pulse oximetry: theory and applications for noninvasive monitoring," Clinical Chemistry, 38, 1601-1607, (1992).

[2] Severinghaus, J.W., "History and recent developments in pulse oximetry," Scandinavian Journal of Clinical and Laboratory Investigation, 53, 105, (1993).

[3] Tromberg, B.J., N. Shah, R. Lanning, A. Cerussi, J. Espinoza, T. Pham, L. Svaasand, and J. Butler, "Non-invasive in vivo characterization of breast tumors using photon migration spectroscopy," Neoplasia, 2, 26-40, (2000).

[4] Doornbos, R.M., R. Lang, M.C. Aalders, F.W. Cross, and H.J. Sterenborg, "The determination of in vivo human tissue optical properties and absolute chromophore concentrations using spatially resolved steady-state diffuse reflectance spectroscopy," Phys Med Biol, 44, 967-81, (1999).

[5] Jobsis, F., "Noninvasive, infrared monitoring of cerebral and myocardial oxygen sufficiency and circulatory parameters," Science, 198, 1264-1267, (1977).

[6] Fishkin, J.B., O. Coquoz, E.R. Anderson, M. Brenner, and B.J. Tromberg, "Frequency-domain photon migration measurements of normal and malignant tissue optical properties in a human subject," Applied Optics, 36, 10-20, (1997).

[7] Dognitz, N. and G. Wagnieres, "Determination of tissue optical properties by steady-state spatial frequency-domain reflectometry," Lasers Med Sci, 13, 55-65, (1998).

[8] Cuccia, D.J., F. Bevilacqua, A.J. Durkin, F.R. Ayers, and B.J. Tromberg, "Quantitation and mapping of tissue optical properties using modulated imaging," J Biomed Opt, 14, 024012, (2009).

[9] Cuccia, D.J., F. Bevilacqua, A.J. Durkin, and B.J. Tromberg, "Modulated imaging: quantitative analysis and tomography of turbid media in the spatial-frequency domain," Opt Lett, 30, 1354-6, (2005).

[10] Bassi, A., D.J. Cuccia, A.J. Durkin, and B.J. Tromberg, "Spatial shift of spatially modulated light projected on turbid media," Journal of the Optical Society of America. A, Optics, Image Science, and Vision, 25, 2833-2839, (2008).

[11] Abookasis, D., C.C. Lay, M.S. Mathews, M.E. Linskey, R.D. Frostig, and B.J. Tromberg, "Imaging cortical absorption, scattering, and hemodynamic response during ischemic stroke using spatially modulated near-infrared illumination," J Biomed Opt, 14, 024033, (2009).

[12] Bassi, A., C. D'Andrea, G. Valentini, R. Cubeddu, and S. Arridge, "Detection of inhomogeneities in diffusive media using spatially modulated light," OPTICS LETTERS, 34, 2156-8, (2009).

[13] Gioux, S., A. Mazhar, D.J. Cuccia, A.J. Durkin, B.J. Tromberg, and J.V. Frangioni, "Three-dimensional surface profile intensity correction for spatially modulated imaging," J Biomed Opt, 14, 034045, (2009).

[14] Konecky, S.D., A. Mazhar, D. Cuccia, A.J. Durkin, J.C. Schotland, and B.J. Tromberg, "Quantitative optical tomography of sub-surface heterogeneities using spatially modulated structured light," Opt Express, 17, 14780-90, (2009).

[15] Belanger, S., M. Abran, X. Intes, C. Casanova, and F.d.r. Lesage, "Real-time diffuse optical tomography based on structured illumination," Journal of Biomedical Optics, 15, 016006, (2010).

[16] D'Andrea, C., N. Ducros, A. Bassi, S. Arridge, and G. Valentini, "Fast 3D optical reconstruction in turbid media using spatially modulated light," Biomedical Optics Express, 1, 471-481, (2010).

[17] Erickson, T.A., A. Mazhar, D. Cuccia, A.J. Durkin, and J.W. Tunnell, "Lookup-table method for imaging optical properties with structured illumination beyond the diffusion theory regime," J Biomed Opt, 15, 036013, (2010).

[18] Mazhar, A., S. Dell, D.J. Cuccia, S. Gioux, A.J. Durkin, J.V. Frangioni, and B.J. Tromberg, "Wavelength optimization for rapid chromophore mapping using spatial frequency domain imaging," J Biomed Opt, 15, 061716, (2010).

[19] Mazhar, A., D.J. Cuccia, S. Gioux, A.J. Durkin, J.V. Frangioni, and B.J. Tromberg, "Structured illumination enhances resolution and contrast in thick tissue fluorescence imaging," J Biomed Opt, 15, 010506, (2010).

[20] Farrell, T.J., M.S. Patterson, and B. Wilson, "A diffusion theory model of spatially resolved, steady-state diffuse reflectance for the noninvasive determination of tissue optical properties in vivo," Medical Physics, 19, 879-888, (1992).

[21] Gioux, S., V. Kianzad, R. Ciocan, S. Gupta, R. Oketokoun, and J.V. Frangioni, "High-power, computer-controlled, light-emitting diode-based light sources for fluorescence imaging and image-guided surgery," Mol Imaging, 8, 156-65, (2009).

[22] Troyan, S.L., V. Kianzad, S.L. Gibbs-Strauss, S. Gioux, A. Matsui, R. Oketokoun, L. Ngo, A. Khamene, F. Azar, and J.V. Frangioni, "The FLARE intraoperative near-infrared fluorescence imaging system: a first-in-human clinical trial in breast cancer sentinel lymph node mapping," Ann Surg Oncol, 16, 2943-52, (2009).

[23] Keller, A., "A new diagnostic algorithm for early prediction of vascular compromise in 208 microsurgical flaps using tissue oxygen saturation measurements," Ann Plast Surg, 62, 538-43, (2009).

[24] Keller, A., "Noninvasive tissue oximetry for flap monitoring: an initial study," J Reconstr Microsurg, 23, 189-97, (2007).

[25] Fang, Q. and D.A. Boas, "Monte Carlo simulation of photon migration in 3D turbid media accelerated by graphics processing units," Opt Express, 17, 20178-90, (2009).
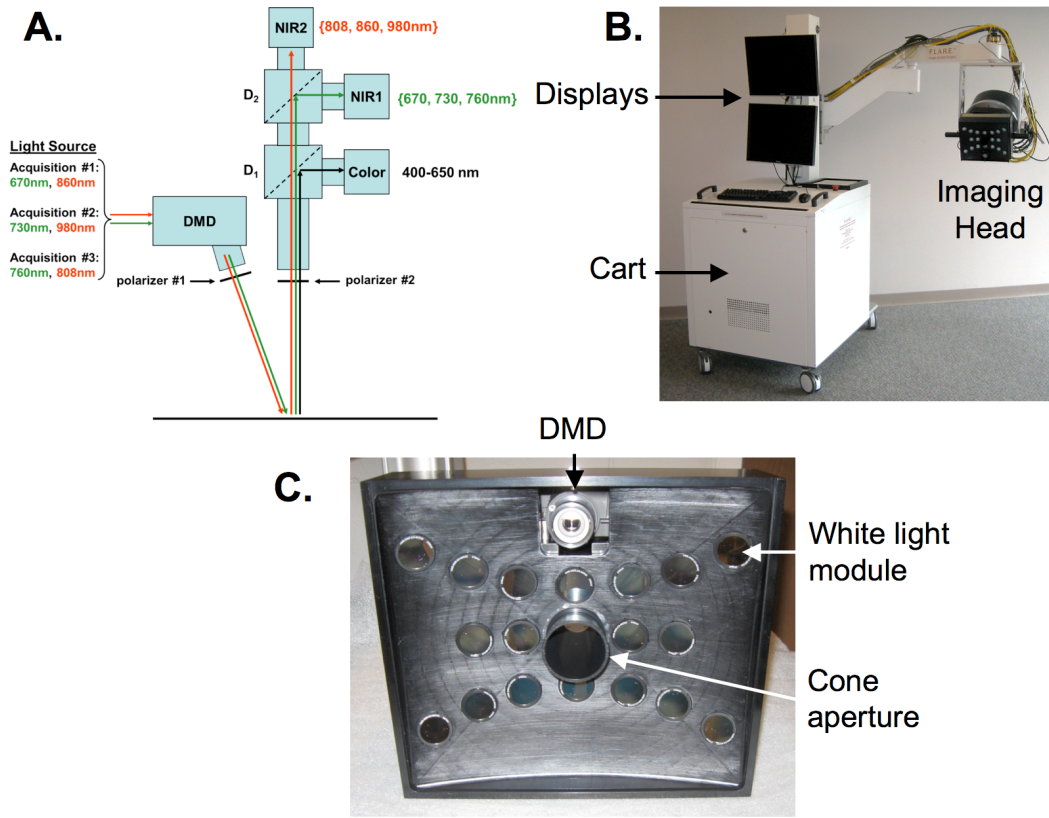
Figure 1: Clinical imaging system working in the spatial frequency domain:
  A. Schematics of the system showing the light paths for all wavelengths into the system imaging head. The light from the NIR light source is propagated to the digital micro-mirror device (DMD) and projected onto the field through a first polarizer. Light is then collected though a second polarizer and split on three cameras using dichroic mirrors.
  B. Picture of the clinic imaging system composed of a cart containing the NIR light source, control electronics, computer, mast, and arm holding the adjustable imaging head.
  C. Bottom view of the illumination section of the imaging head. Note the white light LED modules and the DMD projection optics (upper lens on the picture).
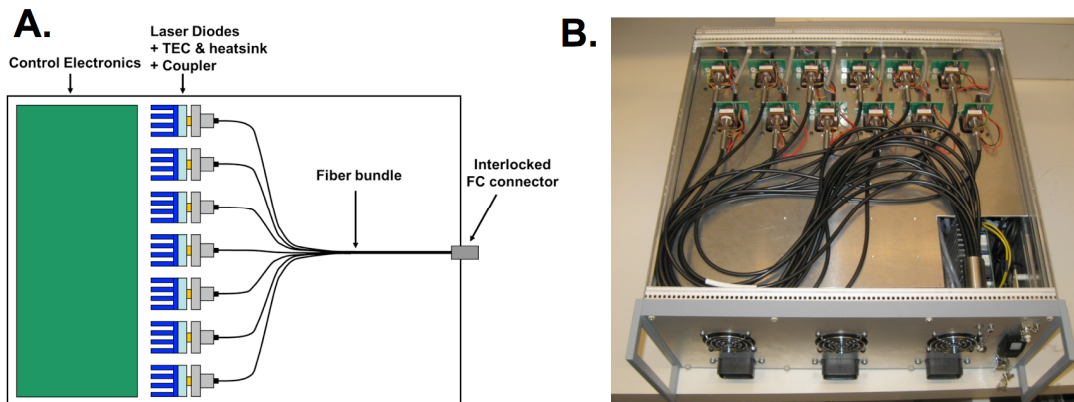

Figure 2: Laser diode based near-infrared (NIR) light source:
  A. Schematics of the NIR light source. Note the control electronics, the wavelength modules composed of one laser diode, and the thermoelectric cooler (TEC) with its heatsink and an interlocked FC coupler. The wavelength modules are combined through a 12-to-1 fiber bundle.
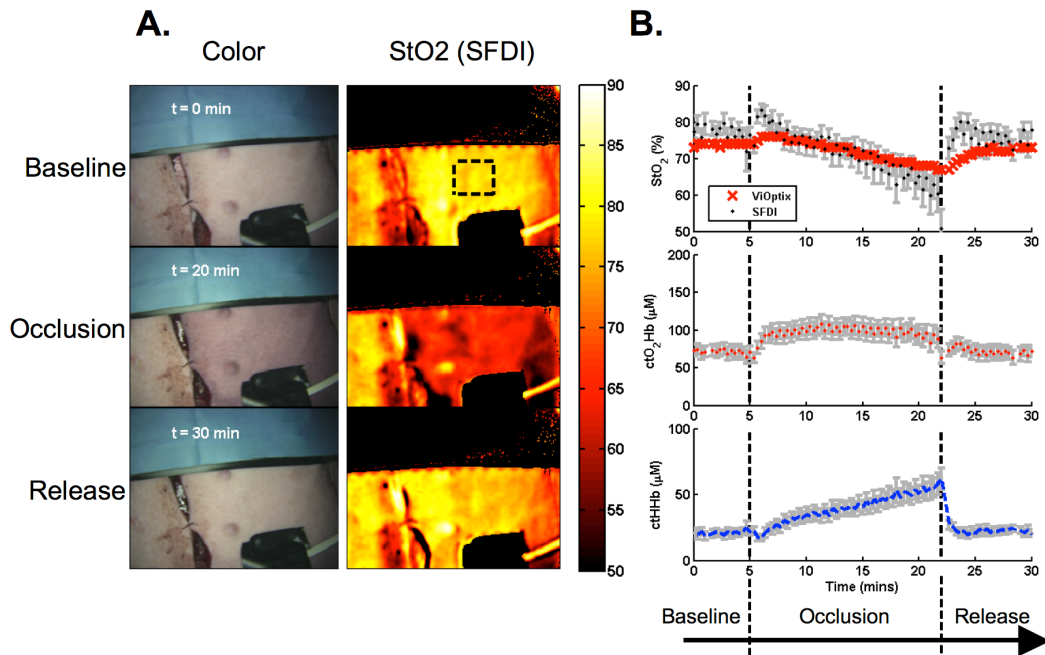 B. Picture of the open NIR light source. Note the wavelength modules and the fiber bundle.

Figure 3: Venous occlusion of skin flap in Yorkshire pig.
- A. Color and SFDI oxygenation images before, during occlusion, and after release, at t = 0, 20 and 30 min respectively. Note a purple discoloration of the tissue during occlusion as blood pools in the tissue. The Vioptix probe can be seen at the bottom right corner of the image.
- B. Oxygen saturation measurements from the SFDI system and Vioptix probe (top), concentrations of oxy-hemoglobin (middle) and deoxy-hemoglobin (bottom) measured by the SFDI system as a function of time. SFDI values are averaged over a region of interest (dashed black square in Fig 3(a)).
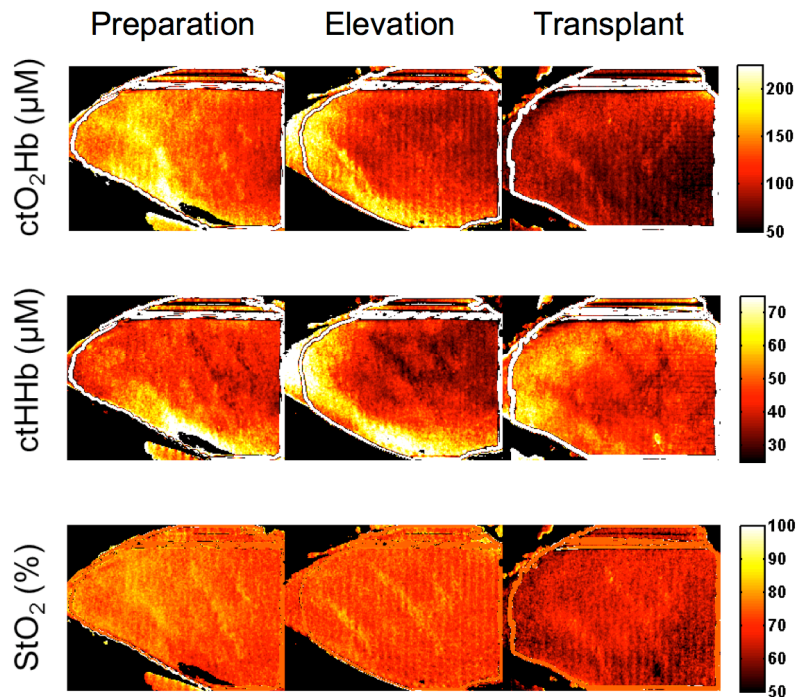

Figure 4: SFDI skin flap oxygenation measurement during the clinical trial. From left to right, preparation of the flap (Preparation), flap after elevation (Elevation), and after surgical attachment (Transplant). Extracted maps of oxyhemoglobin concentration (top), deoxyhemoglobin concentration (middle), and oxygen saturation (bottom) are presented for each step of the procedure. The decrease in oxygen saturation is clearly noticeable in the oxygenation images after transplant.